Renewable and Sustainable Energy Reviews 132 (2020) 110099

Contents lists available at ScienceDirect

Renewable and Sustainable Energy Reviews

journal homepage: http://www.elsevier.com/locate/rser

Techno-economic analysis of a low carbon back-up power system using chemical looping

M.E. Diego *, J.C. Abanades

INCAR-CSIC, Francisco Pintado Fe, 26, 33011, Oviedo, Spain

ARTICLE INFO

Keywords:
Back-up power
Energy storage
CO_2 capture
Chemical looping
Decarbonised electricity
Reactor design

ABSTRACT

This work assesses the techno-economic viability of an innovative CO_2-free back-up power system. A novel chemical looping reactor is at the core of the process, where a pressurized air stream is heated up by the slow oxidation of a packed bed of reduced solids, before its expansion in a gas turbine to generate electricity. In this reactor, air flows through empty gas conducts with fully permeable non-selective perforated walls. Such gas conducts traverse the bed of solids longitudinally, so that the pressure drop is minimized. A diffusionally-controlled flow of oxygen is established through the gas permeable wall, which results in long oxidation times for the bed of reduced particles. A case example is described in this study, where a reactor that uses iron materials as oxygen carrier is designed to store renewable energy (an input of 1.4 MW_{th} of biogas) on a weekly basis and release it to supply a maximum power peak of 57 MW_{th} in the power discharge mode for more than 8 h. A packed bed reactor of 3.3 m I.D. and 50 m length is employed for this application, which is traversed by gas conducts of 0.04 m I.D., with 0.002 m wall thickness and a fraction of orifices in the wall of 0.12. A preliminary economic analysis of the novel system indicates that this low carbon configuration could be competitive against fossil fuel back-up alternatives in several scenarios, preferably with carbon prices exceeding 100€/t CO_2.

1. Introduction

Complete decarbonisation of the power sector is needed to limit the average global temperature increase to 1.5-2 °C, as per the Paris Agreement [1]. Driven by the deep reduction costs achieved by renewables in recent years [2–5], large penetration of renewable energy in the electricity network is anticipated - totalling up to 70% of the electricity generation in 2040 [3]. Integrating high shares of variable renewable energy sources (such as solar and wind) in the electricity grid poses a number of challenges, as they introduce additional variability into the system, which adds up to that associated to daily and seasonal demand fluctuations [2,4,5]. Therefore, a range of flexible and reliable carbon-free back-up power generation technologies are needed in networks largely dominated by renewables [5]. Pumped hydro, and to a lesser extent, Compressed Air Energy Storage, CAES, are viable techno-economic solutions, but they require favourable geographic locations [6]. Currently, peaks in electricity demand are frequently provided by back-up fossil fuel systems such as open-cycle gas turbines, which show a highly flexible performance with moderate capital costs. These peaking gas power plants, also known as "peakers", are built in a range of sizes and operate at average capacity factors as low as 0.04–0.05 (see for example [7,8]). In a CO_2-free scenario, decarbonising such back-up power services using CO_2 capture technologies is a very challenging option [9], because current technical solutions are capital intensive and have limited flexibility. As a result, the capture cost escalates at very low capacity factors. Substitution of fossil fuels by synthetic fuels manufactured from renewable energy is attracting a great deal of R&D interest nowadays [6,10], since *Power-to-Gas-to-Power* or *Power-to-Liquid-to-Power* processes are able to store surplus renewable energy in the form of fuel gases or liquids [2,11]. When the stored gas is electrolytic H_2, underground storage sites (e.g., salt caverns) or large pressurized tanks are needed [12,13]. A high energy-consuming compression step [13], in addition to safety concerns related to H_2 storage at high pressures [14], are the main challenges to deploy such systems for back-up power purposes, especially in densely populated areas. Synthetic fuels containing carbon (e.g. methane, methanol, etc.) can be also produced using carbon-free energy and a source of CO_2 [11,15]. However, the maximum mitigation potential of these processes is limited to 50%, unless the CO_2 comes from the atmosphere, from a biomass source or is recaptured afterwards to close the carbon loop [16]. Furthermore, once that CO_2 has been captured from the atmosphere or

* Corresponding author.
E-mail address: marlen@incar.csic.es (M.E. Diego).

https://doi.org/10.1016/j.rser.2020.110099
Received 27 March 2020; Received in revised form 10 July 2020; Accepted 14 July 2020
Available online 29 July 2020

List of abbreviations

CAPEX	Capital expenditure €/kW
CCF	Capital charge factor
CF	Capacity factor
COE	Cost of electricity €/MWh_e
E_{CO2}	CO_2 emission rate t CO_2/MWh_e
$E_{CO2\ ref}$	CO_2 emission rate of the reference system t CO_2/MWh_e
$OPEX_{fixed}$	Fixed operating costs €/MW
$OPEX_{var}$	Variable operating costs €/MWh_e
TTF	Multiplier to obtain the total as-spent capital using the total plant cost

fixed by photosynthesis in the form of biomass, there are negative emission options competing with the neutral synthetic fuel routes [17].

In this work, we investigate the technical and economic viability of a novel carbon-free alternative for some of the energy storage/back-up power services of the future. A novel chemical looping combustion (CLC) reactor recently proposed by the authors for CO_2 capture systems [18] is at the core of the process. The similarity of the proposed system with existing back-up power systems using gas turbines is exploited in this study to present a basic cost analysis that establishes the conditions (i.e., the carbon price) at which this carbon-free power system could be competitive with respect to a fossil fuel-based benchmark.

2. Process concept

The proposed system is conceived as a thermochemical energy storage concept (see Fig. 1) that exploits chemical looping combustion principles of reversible redox reactions taking place at high temperatures, while maintaining a process scheme similar to that of an existing gas turbine power system. This similarity will facilitate a transparent cost analysis of this option, by comparing it against well-established benchmarks to deliver the same back-up power service burning fossil fuels today.

As can be seen in Fig. 1 (left), a novel chemical looping reactor is at the core of the process and is the key element to assess the techno-economic viability. This reactor will alternate between charging and discharging stages to provide energy storage and back-up power capability. During energy discharge periods (red flow lines in Fig. 1 (top left)), a bed of solids is slowly oxidized by means of a diffusionally-controlled flow of oxygen [18], in order to deliver a pressurized gas stream at high temperature that can be expanded in a downstream turbine to generate electric power. During charging periods (Fig. 1 (bottom left), blue flow lines), energy in the form of a renewable fuel gas (H_2, biogas, etc) is used to reduce the oxidized batch of solids. Details on turbomachinery, auxiliary cycle elements (such as heat recuperators, air preheaters or heat recovery steam generators) to increase energy efficiencies, or even advanced cycle concepts where there is no mechanical connection between compression and expansion (i.e., like in CAES) are considered out of the scope of this work. They are simply assumed to be the same in the novel system as in the benchmark option used for the techno-economic study (see section 4 below).

A first condition for the reactor of Fig. 1 (top left) is to contain a sufficiently large mass of reduced material (*Me* in the figure, to be oxydized to *MeO* by air). Therefore, candidate *Me/MeO* oxygen carrier materials should be available at low cost and have very high theoretical energy storage density. This is the case of e.g. Fe/Fe_2O_3 or $CaS/CaSO_4$, whose enthalpy of full oxidation is 7440 kJ/kg Fe and 13,320 kJ/kg CaS, and particle density is 7874 and 2590 kg/m^3, respectively. A second condition for the reactor is to be able to operate at the high pressures (>10 bar) and temperatures (>1000 °C) usually required in Brayton power cycles. This is a major known barrier for chemical looping air reactors using a packed bed configuration, as very sharp oxidation reaction fronts appear when the bed of solids is oxidized with air [19–21], with maximum temperatures that will compromise the integrity of the material. Diluting the active part of the oxygen carrier with a large fraction of inert material [22,23] or arranging large N_2 recycles to the bed [24,25] have been proposed as suitable solutions for fast switching CLC reactor systems using packed beds. However, they are impractical in this application, because the energy storage density would decrease accordingly when diluting the effective oxygen carrying capacity of the bed. Also, the oxidation/reduction cycle time scales in CLC packed bed systems are in the range of minutes [22–25], which is insufficient for back-up power applications, where several hours of power discharge may be needed. On the other hand, alternative CLC set ups involving fluidized bed of solids with continuous feed of *Me* and discharge of *MeO* are left outside the scope of this work, as these would likely be uneconomic for the low capacity factors expected for back-up power systems.

Fig. 2 presents a schematic of the novel air reactor that has been

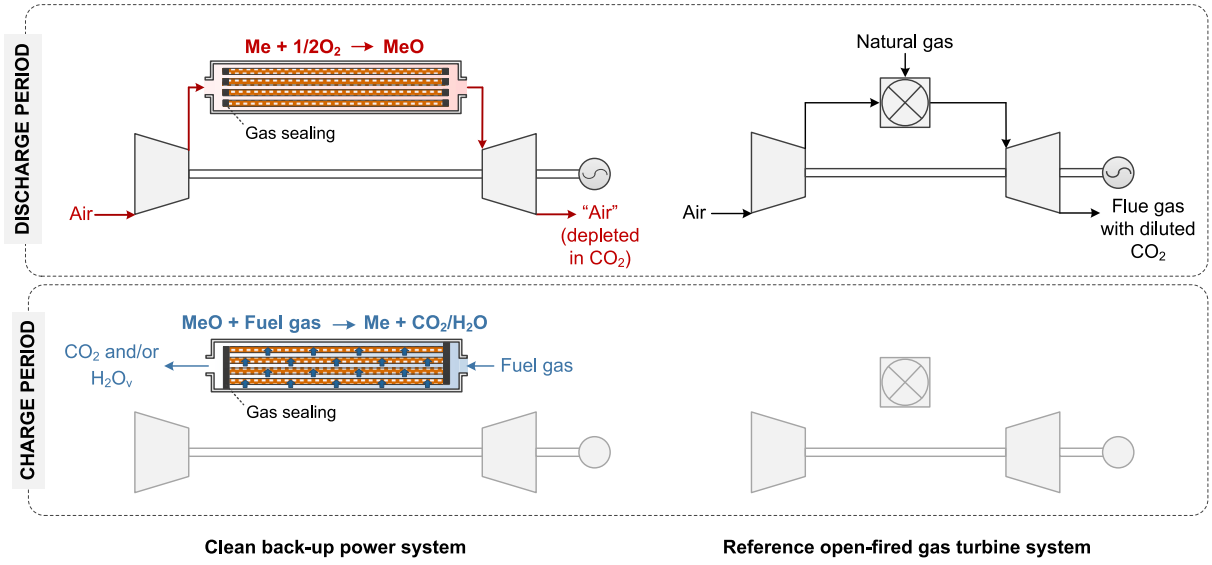

Fig. 1. The back-up power concept proposed in this work (left) and the reference open-fired gas turbine system considered as a benchmark (right). The top figures represent power discharge periods while those at the bottom represent charging periods.

recently proposed by the authors [18] to overcome these limitations and allow a controlled oxidation of a large batch of *Me* to *MeO* with air. A key difference with previous air reactor designs is to impose a diffusion-controlled step to the overall oxidation reaction, so that the whole batch of solids in the reactor is forced to react in an atmosphere extremely depleted in oxygen (see schematics in Fig. 2). For this purpose, the packed bed of solids is traversed longitudinally by gas conducts, which are free of solids and open at both ends, so that pressure drop of the air flow passing through the reactor is minimized. Note that there is no direct convective flow of air through the solids in this set up. The gas in the vicinity of the solid particles is "stagnant" (i.e. mass transport is only allowed by a diffusion mechanism in the bed of solids).

The gas conducts, which occupy the entire length of the reactors, have thin perforated walls (metallic in the examples below) to separate the air flow and the beds of solids, so as to avoid direct contact between the gas and the oxygen carrier particles. In this set-up, the gas and the solids remain at the same high pressure in both sides of the walls (see Fig. 2). The gas conduct walls are, therefore, fully permeable and non-selective to gases, as well as thermally conductive to allow the energy generated by the oxidation of the solids to flow to the air passing through the conducts. At the high temperatures of operation, the solid particles in the packed bed will have a great affinity to react with oxygen. Hence, solids are forced in this set-up to share the limited oxygen supply arriving by diffusion from the oxygen-rich air flow passing through the gas conducts. The size of the orifices in the gas conduct walls is assumed to be sufficiently small so as to avoid solids entering the gas region. In such conditions, Fick's diffusion law is assumed to govern the flux of oxygen through the orifices, hence limiting the overall oxidation rate, as long as the oxidation kinetics of the oxygen carrier particles is sufficiently fast as to maintain the O_2 partial pressure in the voids between the particles close to zero (gas is stagnant around the bed of solids in Fig. 2). Since the overall oxidation rate is deliberately slowed down in this configuration, the reactor can be designed so that only a small conversion of the total inlet flow of oxygen takes place when reacting with the solids. Indeed, a large bypass of air in the reactor is an essential feature of the system during the oxidation stage, since low O_2 gas conversion is needed to moderate adiabatic oxidation temperatures. Such conversion of oxygen can be arranged to match the necessary heat transfer required to heat up the high-pressure air flowing through the gas conducts to the required reactor exit temperature (see case study below and elsewhere [18]). It should be noted that a net diffusion of N_2 from the stagnant gas towards the gas conducts is not expected to occur in the reactor despite the concentration gradient, as it would demand the same gas flow in the opposite direction to maintain the equal gas pressure in both sides of the permeable wall.

At the end of the discharge period, a charge period (or reduction stage) must be accomplished using a reducing gas, which can be chosen from a range of options. It should ideally be a renewable clean fuel gas such as biogas, biomass syngas or renewable H_2. Fossil origin natural gas could be also a suitable technical option for reducing the solids, as long as emission of the highly-concentrated CO_2 generated during the slow reduction stage can be avoided. In any case, the reduction of the oxygen carrier with a fuel gas could take place inside the reactor by changing the gas-solid contacting mode, as can be seen in Fig. 1 (bottom left). Fuel bypass has to be minimized during the reduction stage to achieve a high gas conversion. To this end, the reducing gas is only fed through the gas conducts located at the bottom of the reactor, while blocking all other inlets and outlets, except the outlets of the gas conducts located at the top of the reactor (see Fig. 1). Therefore, the fuel gas is forced to pass through the entire bed of solids by exploiting the full permeability of the orifices in the conduct walls. In such arrangement, the permeable walls act as a gas distributor/diffuser and there is a fully convective flow of gas through the packed bed of solids, hence minimizing any bypass of the fuel to the exit. As the reduction step progresses, a continuous stream of water vapour (if H_2 or CH_4 is selected as reducing agent) and/or CO_2 (when a carbon-containing reducing gas is used) is generated, which ultimately leaves the reactor through the gas conducts located at the upper part of the reactor (see Fig. 1 (top)). It is important to note that the reduction step can take place slowly during long periods of time in between discharge periods. Therefore, the main focus of this work will be, from now on, the power discharge oxidation stage, which is the most challenging stage and the main driver to take reactor design decisions.

3. Design case study

A chemical looping reactor that employs biogas as reducing agent has been chosen to illustrate the potential of the thermochemical energy storage system proposed in this work. The reactor is designed to supply a maximum power peak of 20 MW_e, which corresponds to about ~57 MW_{th} assuming an electrical efficiency of 35%, similar to that found in small commercial gas turbines for power generation (e.g. Refs. [26,27]). A range of oxygen carrier materials could be used in the reactor (e.g. Fe-based, $CaS/CaSO_4$, Ni-based etc), and the final oxygen carrier material choice will depend on its cost, the specific application and the operating conditions of the process. In this example, iron is employed as functional material in the oxygen carrier, since it is an inexpensive material with high theoretical volumetric oxygen transport capacity and is stable at temperatures over 1000 °C. Other oxygen carriers could have also been considered to illustrate the concept, which could overcome some of the known limitations of iron-based materials (e.g., agglomeration of Fe particles and equilibrium constraints during oxygen carrier reduction). The system is conceived to store renewable energy on a weekly basis, and operate in the power discharge mode with a capacity factor of 0.05. For this purpose, a continuous flow of biogas (222 Nm^3/h - 65%vol. CH_4, 35%vol CO_2 [28] -, equivalent to that employed in a medium-size biogas power plant [29]) is used to reduce a batch of Fe_2O_3 oxidized solids. During this stage, Fe_2O_3 will sequentially reduce to Fe_3O_4, FeO and Fe in several reaction fronts as biogas is fed to the bed. Assuming no kinetic restrictions are in place (the reduction stage can take place with a small flow rate of fuel during the week-long periods in

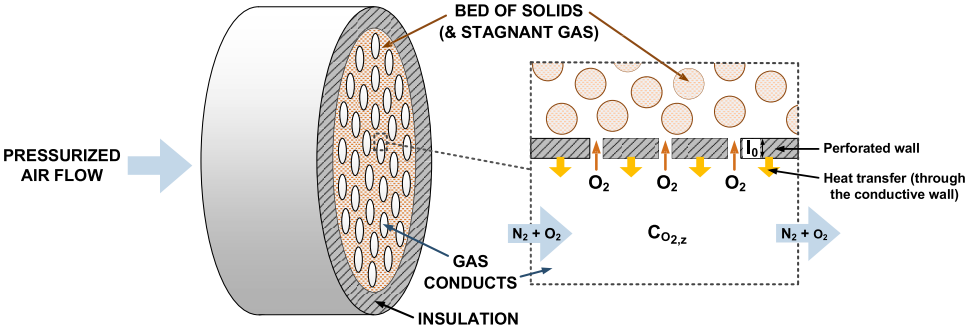

Fig. 2. Schematics of a thin slide of the reactor of Fig. 1 (top) and detail of the main oxygen and thermal fluxes in the vicinity of the gas conduct walls.

Table 1
Boundary conditions and main assumptions of the case study.

Design system discharge power	MW_e	20
Electrical efficiency	η_e	0.35
Gas conducts and reactor length	m	50
Internal diameter of the gas conducts, D_c	m	0.04
Thickness of the perforated wall, l_0	m	0.002
Fraction of wall area occupied by orifices in the perforated wall, ε_w	–	0.12
Air inlet temperature to the reactor	°C	500
Air inlet pressure to the reactor	bar	15
Inlet velocity of air in the conducts	m/s	15
Capacity factor		0.05
Oxygen carrier	–	$Fe/FeO/Fe_3O_4/Fe_2O_3$ system
Volume fraction of active oxygen carrier	–	0.3
Average oxygen transport capacity of the oxygen carrier	kg O_2/kg Fe_2O_3	0.136
Average bed oxidation enthalpy to Fe_2O_3	kJ/mol O_2	547
Density of the reduced (average)/oxidized solids	kg/m^3	5962/5250
Reducing agent	–	Biogas (65%vol. CH_4, 35%vol CO_2)
Biogas flow (charge period)	mol/s	2.8[a]
Duration of the charge (storage) stage	days	7

[a] Calculated flow generated in a 568 kW_e biogas plant, assuming 40% efficiency for the electricity generation [29], biogas composition of 65/35%vol. CH_4/CO_2 and LHV = 20 MJ/kg [28].

between the power discharge cycles linked to the oxidation stage of the oxygen carrier), biogas will first reduce FeO particles to Fe until equilibrium is reached. The equilibrium gas composition leaving that reaction front will then come into contact with Fe_3O_4 particles, which will be reduced to FeO. Finally, the equilibrium gas composition leaving this reaction front will reduce the Fe_2O_3 solids to Fe_3O_4. Complete conversion of the fuel can be achieved under relevant reduction conditions when Fe_2O_3 reduces to Fe_3O_4, hence leading to a highly-concentrated CO_2 stream (after H_2O condensation). Therefore, the reactor charge stage is stopped when the last mole of Fe_2O_3 is converted back to Fe_3O_4 to avoid any unconverted fuel leaving the reactor, which would dilute the CO_2/H_2O exiting stream. As a result, a mixture of iron solids with different oxidation states is obtained at the end of the charging step, which will be oxidized back to Fe_2O_3 afterwards during the power discharge stage. The proportion of $Fe/FeO/Fe_3O_4$ in the reduced bed has been calculated in this work taking into account the equilibrium restrictions of the Fe_2O_3/Fe_3O_4, Fe_3O_4/FeO and FeO/Fe systems using the HSC software. The gaseous species CH_4, CO_2, CO, H_2, H_2O and O_2 have been considered in these calculations (as in Jerndal et al. [30]), using the biogas composition shown in Table 1 and assuming reduction takes place at an average temperature of 700 °C and 1 bar. The calculated molar fraction of Fe, FeO and Fe_3O_4 in the reduced bed employing this procedure is 0.19, 0.80 and 0.01, respectively. It is important to note that reduction of the solids with the CH_4 contained in the biogas will translate into a substantial reduction in the temperature of the bed (the average enthalpy of reduction of the previous oxide mix is ~150 kJ/mol O_2). However, it should be possible to maintain higher average reduction temperatures of the solids (more favourable for reduction equilibrium and kinetics) if brief oxidation stages were introduced with the sole purpose of reheating the bed of solids during the week-long reduction stage. However, the analysis of such dynamic intermediate oxidation periods is considered outside the scope of this work.

As illustrated in Fig. 1, the novel energy storage/back-up configuration presented in this study can be benchmarked against a reference system consisting of a 20 MW_e open gas-fired cycle that also operates as peaking power plant at low capacity factor (0.05) [7]. The main assumptions and design parameters used as inputs in this work are presented in Table 1, whilst the Appendix compiles a summary of the reactor design rules described in more detail elsewhere [18]. In this case study, air is assumed to enter the reactor at 500 °C and 15 bar. Gas conducts with internal diameter of 0.04 m and 50 m of effective length are considered for this application, whereas the inlet velocity of the air entering the conducts is 15 m/s. Furthermore, the thickness and fraction of orifices of the perforated gas conduct walls is set at 0.002 m and 0.12, respectively. For the calculations, O_2 diffusivity is estimated using correlations as reported in Ref. [31]. The fraction of active oxygen carrier material in the bed is fixed at 0.3 (volume), in order to ensure there is enough space in the bed to accommodate a porous support as well as volume changes of the oxygen carrier during oxidation. For the sake of simplicity, average bed properties (oxygen transport capacity, oxidation enthalpy, solids density) have been used for the oxidation calculations of the oxygen carrier particles. These have been obtained taking into account the proportion of $Fe/FeO/Fe_3O_4$ present in the reduced bed (the values are summarized in Table 1).

The design results and main outputs of the simulated reactor are presented in Table 2. As can be seen, an energy storage capacity of 490 MWh_{th} is calculated for the reactor under the design conditions described above. In this set-up, the reactor is able to deliver a flow of hot pressurized gas at 1100 °C and 14.7 bar that will ultimately be used to drive a downstream gas turbine to generate a CO_2-free power peak of 20 MW_e. This is achieved using a total of 634 gas conducts that traverse the bed of solids, each one surrounded by a packed bed of reduced oxygen carrier material with a thickness of 0.043 m. These can be arranged in a reactor of 3.3 m inner diameter and 50 m length, which has an energy density of 1177 kWh_{th}/m^3. Alternative layouts with u-tube gas conducts shape might be also considered, where the total reactor length is reduced at the expense of a larger diameter. Moreover, it has been calculated that the reactor can operate intermittently for a minimum time of 8.8 h until complete oxidation of the iron solids in the packed bed reactor takes place.

The calculated gas and wall temperature profiles at the beginning of the oxidation period are shown in Fig. 3, which also depicts the variation of the O_2 molar fraction as a function of the reactor length. An almost linear trend is obtained in all cases, since the oxygen flux is similar at any point along the reactor (see Table 2). As discussed elsewhere [18], this is due to the opposite effects of temperature on diffusivity and concentration of O_2, which nearly compensate, hence leading to similar values of the oxygen flux (see equation A.1 in the Appendix). It is important to note that, if higher turbine inlet temperatures were necessary, the Brayton cycle could be top up by burning a fuel gas at the exit of the reactor. This could also be an option to offset the effects of the additional diffusion resistance that might appear as the oxidation front departs perpendicularly from the gas conduct wall as the discharge stage progresses, which can be also compensated for by employing multireactor configurations, hence contributing to maintain a stable power output (this has not been taken into account in this work for the sake of simplicity, but more details can be found in Ref. [18]). In any case, burning a fuel gas would be at the expense of an increase in the system's

Table 2
Summary of parameters at the beginning of the discharge (oxidation) stage.

Energy storage capacity	MWh_{th}	490
O_2 diffusivity, D_{O2} (inlet/outlet)	m^2/s	$7.2{\cdot}10^{-6}$/ $1.9{\cdot}10^{-5}$
Initial flux of O_2 through the orifices (inlet/outlet)	mol/m^2s	0.18/0.23
Local heat transfer coefficient of the wall, $h_{w,z}$ (inlet/outlet)	W/mK	317/417
Molar fraction of O_2 at reactor outlet		0.181
Gas temperature at reactor outlet	°C	1100
Pressure drop of the gas in the reactor	bar	0.3
Thickness of the solids bed surrounding gas conducts	m	0.043
Number of gas conducts		634
Equivalent internal diameter of the reactor	m	3.3
Energy density	kWh_{th}/m^3	1177
Minimum time for the complete oxidation of Fe particles	h	8.8

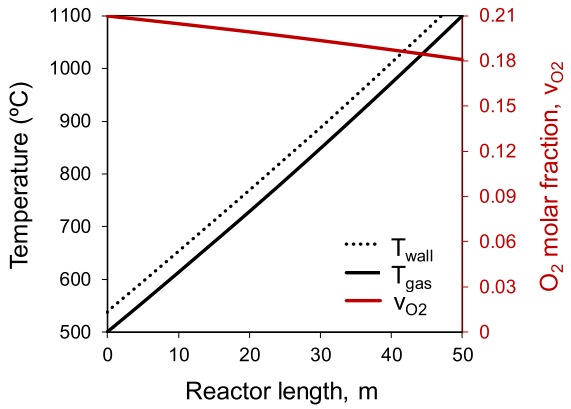

Fig. 3. Initial gas and wall temperature profiles and variation of the O_2 molar fraction as a function of reactor length.

carbon footprint, which could be minimized if a renewable fuel gas is employed.

The results obtained in this section show that the use of biogas as reducing agent during the charge stage allows the reactor to store low-power renewable energy that will be discharged afterwards in the form of a large 20 MW_e power peak. It is important to note that alternative gases different from biogas can be used for the charge (reduction) stage. However, biogas has been chosen here as a particularly interesting renewable opportunity fuel, which allows carbon-free electricity to be supplied during discharge periods, whilst generating a continuous stream of highly-concentrated CO_2 (after H_2O condensation) that can be integrated in future large CCS or CCU networks. This provides an additional advantage to the system represented in Fig. 1 (left), as it could lead to net negative carbon emissions using a renewable gas, which would otherwise be burnt to generate electricity, hence emitting CO_2. Nevertheless, specific challenges arise when biogas is used as reducing agent. Carbon deposition can occur during the charging stage, which should be minimized to lessen carbon leakages when the oxygen carrier is oxidized. Moreover, reducing the oxygen carrier using biogas can lead to a large temperature decay in the bed if no action is taken due to the high associated reduction enthalpy. As mentioned above, strategies could be adopted to offset this effect, such as performing short oxidation stages with the sole purpose of reheating the bed of solids during the week-long reduction stage. Analysis of the transient states of the system and detailed heat management strategies is considered out of the scope of this study, which should be investigated in future works aiming at developing this concept further. Moreover, it is important to note that the large volume/surface ratio of the reactor, together with standard thermal insulation methods, makes this reactor quasi-adiabatic for the time scales under discussion. Hence, once the reduction stage finishes, the temperature of the solids can be assumed to be maintained even if the oxidation step does not start immediately afterwards, as very low heat losses can be expected from the pile of stationary solids.

4. Economic analysis

We present in this section a first economic assessment of the concept using a recent methodology proposed by Guandalini et al. [32] to estimate the cost of emerging CO_2 capture technologies. This is especially suitable for novel technologies sharing key cost elements with well-established commercial benchmarks, as it is the case here (see Fig. 1). In this method, a clear distinction is made between those elements in the system that are mature and well characterized in terms of performance and cost, and the novel components. Instead of calculating the equipment cost related to the novel components and adding it up to that of the known equipment, this methodology calculates the equipment cost allowed for the novel elements (cost gap) in order to make the process competitive against the benchmark system [32]. This is particularly important to assess the techno-economic viability of a full new system: if the cost gap allowed for the novel chemical looping reactor equipment is large, there may be room to accommodate uncertainties and contingencies related to the novelty of the system. If the cost gap is tight, the novel process is unlikely to be competitive respect to the benchmark when considering such contingencies.

The energy storage/back-up system presented in this work is benchmarked here against an open gas-fired cycle that has exactly the same capacity and operates at an identical capacity factor. As depicted in Fig. 1, both systems make use of the same commercial elements (compressor, turbine, heat exchangers, generator) that are already available at competitive costs, whilst the combustor is replaced by the novel chemical looping reactor in the new system. In order to estimate the cost gap of the reactor equipment that makes the back-up system competitive with the reference gas turbine, the difference in the cost of electricity (ΔCOE) between the novel concept and the benchmark is defined as:

$$\Delta COE = \frac{\Delta CAPEX \cdot TTF \cdot CCF + \Delta OPEX_{fixed}}{8760 \cdot CF} + \Delta OPEX_{var} + \Delta Fuel\ cost = Cost\ of\ CO_2\ avoided \cdot \left(E_{CO_2\ ref} - E_{CO_2}\right) \quad (1)$$

where ΔCAPEX, $\Delta OPEX_{fixed}$ and $\Delta OPEX_{var}$ represent the difference in terms of capital, fixed and variable operating costs, respectively, between the novel concept and the benchmark system, TTF is a multiplier used to obtain the total as-spent capital (TASC) using the total plant cost (TPC) [32], CCF is the capital charge factor, CF represents the capacity factor, $E_{CO2\ ref}$ is the CO_2 emission rate of the reference system and E_{CO2} is that of the novel configuration proposed.

As discussed above, the only element that contributes to the difference in capital costs between the back-up and the reference system is the novel reactor. Therefore, $\Delta CAPEX = CAPEX_{reactor}$ in equation (1) when making the assumption that the reactor replaces the combustor in an open cycle gas turbine that is already amortized (otherwise $\Delta CAPEX = CAPEX_{reactor}\text{-}CAPEX_{combustor}$). Moreover, fixed operating costs include labor, taxes and insurances, which are here assumed to be the same as in the benchmark plant, i.e., $\Delta OPEX_{fixed} = 0$. Differences in variable operating costs are, in turn, attributed to variations in maintenance and consumable costs. Nevertheless, it is assumed that additional consumables are not needed for the operation of the reactor due to the long lifetime envisaged for the oxygen carrier particles when the system operates at very low capacity factors (for comparison, a lifetime of 5 years is typically assumed for oxygen carriers that experience a high number of reduction-oxidation cycles in chemical looping systems working at high capacity factors, e.g. Ref. [33,34]). Besides, the higher maintenance costs that could be expected in the system of Fig. 1 (top) are assumed to be offset by the by-product credit that could be obtained by selling the continuous stream of highly-concentrated CO_2 (after H_2O condensation) obtained during the reducing (charge) stage. Therefore, $\Delta OPEX_{var}$ is also taken to be zero in this preliminary cost analysis. The last term in equation (1) is related to fuel cost, which is associated to the biogas employed during the charge stage and to the natural gas used for combustion in the case of the novel reactor and the benchmark plant, respectively. Other assumptions and parameters used in the economic analysis are shown in Table 3.

A break-even line is depicted in Fig. 4 (in red) using equation (1) and the assumptions discussed above. This line separates the economically competitive (red shaded) and uneconomic (white) regions of the novel back-up system with respect to the benchmark open gas turbine configuration, as a function of the capital expenditure dedicated to the reactor and the maximum allowed cost of CO_2 avoided. In order to take into account possible variations in fuel price and/or any subsidies associated to the use of clean fuels such as biogas, two additional break-even lines are represented in the figure, assuming that the difference in

Table 3
Summary of parameters and assumptions employed in the economic analysis.

TPC-to-TASC factor, TTF	–	1.32[a]
Capital charge factor, CCF	%/yr	10.88
Capacity factor, CF	–	0.05
Natural gas price	€/GJ_{LHV}	4[b]
Biogas cost	€/GJ	5[c]
$\Delta OPEX_{fixed/var}$	–	0
$E_{CO2\ ref}$	t_{CO2}/MWh_e	0.578
E_{CO2}	t_{CO2}/MWh_e	0

[a] Calculated as the average value used for natural gas combined cycle power plants from DOE/NETL [35].
[b] Consistent with reference [36].
[c] Consistent with the central value of the interval reported by IRENA (0.11–0.50$/$m^3$ CH_4) [37], calculated considering the oxidation heat of previously reduced iron solids using biogas.

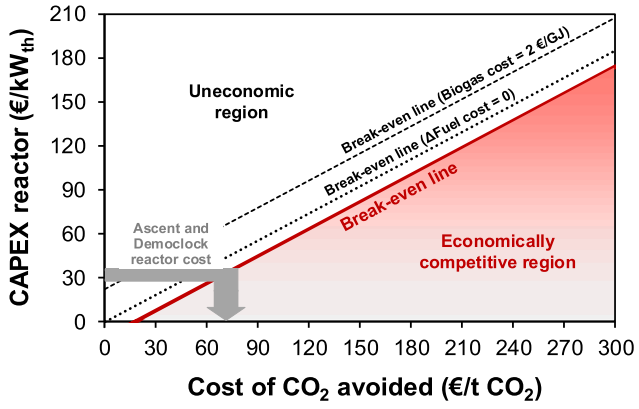

Fig. 4. Representation of the break-even line (in red) that shows the combinations of reactor capital and CO_2 avoided costs (carbon price) that make the novel back-up system economically competitive in comparison to a benchmark open gas-fired turbine using the values of Table 3. The black dotted line illustrates the break-even line when there is no difference in fuel costs between the back-up configuration and the benchmark, whereas the dashed-line illustrates the break-even line for a biogas price of 2 €/GJ. The cost range of pressurized packed bed reactors for chemical looping purposes is shown in grey using the information given by Mancuso et al. [33] and Riva et al. [34]. (For interpretation of the references to colour in this figure legend, the reader is referred to the Web version of this article.)

the fuel cost is zero between the new system and the benchmark (black dotted line) and that the cost of biogas is 2 €/GJ (black dashed line representing the lower cost limit reported in Ref. [37]). For the sake of comparison, the cost of a pressurized chemical looping reactor per unit of thermal power operating in a packed bed configuration is also included in Fig. 4 (grey thick line), using the information reported in recent economic studies carried out in the framework of two reference projects: Democlock [33] and Ascent [34]. According to these assessments, reactor capital costs of 28–35 €/kW_{th} [34] (for the 25 and 11 bar case, respectively) and 32 €/kW_{th} [33] can be calculated, when the fraction of the total equipment cost associated to the oxidation reactors is considered. These values can be taken as a first reference of the expected costs of the novel reactor, which would be in the 1.6–2.0 M€ range for the case example considered in this work. However, there are obvious differences in the arrangement of the reactors that will affect the cost of the novel reactor and hence, the break-even carbon price. Unlike "conventional" chemical looping systems, the novel back-up/energy storage reactor contains a number of gas conducts with perforated walls that traverse the packed bed of solids, hence increasing the reactor cost. Nevertheless, this reactor does not necessitate some of the elements required in pressurized packed bed reactors for "conventional" chemical looping, such as the set of high-temperature switching valves, whose costs are included in the reference values given by Riva et al. [34].

As can be seen in Fig. 4, the cost gap allowed for the novel reactor directly depends on the carbon price allocated for decarbonized back-up power services. If the reactor capital costs reported in the Democlock and Ascent projects are taken as reference, it can be calculated that carbon prices above 64–75 €/t CO_2 (46–57 €/t CO_2 if ΔFuel cost = 0) would be required to make the novel back-up system of Fig. 1 (left) economically competitive with respect to open cycle gas turbines using fossil natural gas. Any increase in the cost of the novel chemical looping reactor with respect to these reference values would lead to higher costs of CO_2 avoided using the back-up system assessed in this work. It is important to highlight that despite the required carbon prices that make the novel back-up reactor competitive with gas-fired open cycle turbines may seem high, decarbonising discontinuous sources such as back-up power plants is particularly difficult and undoubtedly more costly than cutting CO_2 emissions from any continuous process, especially when the former operate at low capacity factors. Besides, the values shown in Fig. 4 do not incorporate additional reductions in the cost of CO_2 avoided that will arise if the continuous highly-concentrated CO_2 flow (after H_2O condensation) generated during the reducing stage is not used but integrated in a future CCS network for permanent storage. The effects of this option, which leads to net negative CO_2 emissions, as well as those of an increase in the capacity factor on the economics of the novel back-up/energy storage concept are illustrated in Fig. 5.

Changes in the break-even line as a result of increasing the capacity factor of the back-up and benchmark systems from 0.05 to 0.10 and 0.20 are represented in Fig. 5, whilst keeping the values of other variables unchanged. As expected, the capacity factor has a large influence on the break-even line (see Equation (1)), and moderate rises in the capacity factor lead to a substantial increase in the reactor cost gap allowed for a certain carbon price. In fact, if the costs of reactor equipment from Ascent and Democlock projects are taken into account, the carbon price needed to make the novel back-up system competitive with the benchmark would decrease from 64-75 €/t CO_2 to 41–46 and 29–32 €/t CO_2 when the capacity factor increases from 0.05 to 0.10 and 0.20, respectively. The implications of a system with negative CO_2 emissions (E_{CO2} = −0.427 t CO_2/MWh_e) are also shown in Fig. 5, assuming CO_2 transport and storage costs of 8 €/t CO_2 (consistent with [35]). As can be seen, the break-even line shifts significantly towards the left also in this case where the capacity factor is 0.05. As a result, the economically competitive area of the novel system is enlarged for a certain carbon price, hence increasing the margin available to accommodate uncertainties and contingencies related to the novelty of the system.

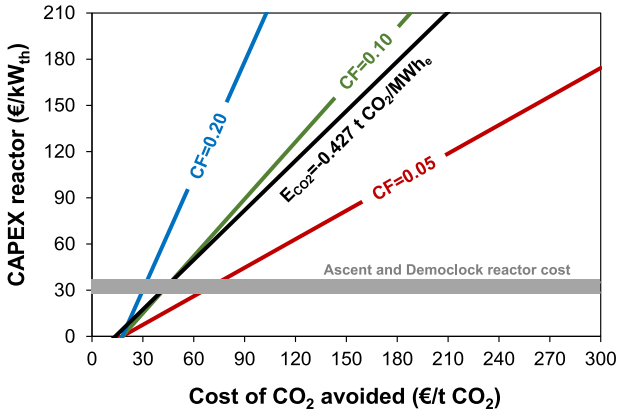

Fig. 5. Sensitivity analysis of the effect of changes in the capacity factor (CF) of the novel back-up system (and its benchmark) on the break-even line. The black line represents the break-even line obtained when the CO_2 from the charge stage is permanently stored (negative CO_2 emissions) and the capacity factor is 0.05.

The preliminary economic analysis carried out in this work shows that there is room for competitiveness of the novel back-up/energy storage system presented here with respect to traditional fossil fuel alternatives. Interesting opportunities can exist for this system, which may require designing the back-up system to operate at moderately low capacity factors (e.g., 0.10) or under a full CO_2 capture and storage configuration in scenarios of moderate carbon prices.

5. Conclusions

The techno-economic viability of an innovative energy storage/back-up power system that employs a novel chemical looping reactor has been assessed in this work. This configuration allows storing large amounts of renewable energy for long periods of time and supplying CO_2-free electricity pulses during peak demand periods, hence serving as balancing asset for renewables. First reactor design calculations show that an initial power peak of 57 MW_{th} (equivalent to 20 MW_e with 35% cycle efficiency) can be generated by slowly oxidizing a bed of reduced Fe solids in a reactor of 3.3 m I.D. and 50 m length, using a total of 634 gas conducts of 0.04 m I.D. with wall thickness of 0.002 m and a fraction of orifices per wall area of 0.12, under the conditions assumed in this study. The oxidation heat released is used to heat up a pressurized air flow, which leaves the reactor initially at 1100 °C and 14.7 bar (pressure drop is of only 0.3 bar) and is subsequently expanded in a gas turbine to produce carbon-free electricity. The reactor, which replaces the combustor in gas turbine configurations, can be used intermittently to produce power for more than 8 h. At the end of the discharge period, the oxidized solids can be reduced inside the reactor during the long times in between discharge (oxidation) cycles using biogas, although other fuel gases can be also employed for this stage. If the reducing gas contains carbon (as it is the case of biogas), a continuous stream of highly-concentrated CO_2 is obtained during the charge period, which could be integrated in a larger CO_2 transport and permanent storage network or intended for other uses. A competitive cost can be expected for the configuration analysed in this work, since the reactor has no moving parts and the specific cost of the functional materials is low, whilst the remaining elements in the system (compressor, turbine, heat exchangers, generator) are mature technology already available at moderate costs. A preliminary economic analysis of the proposed system shows that it could be competitive with respect to a benchmark open-cycle gas turbine configuration even at very low capacity factors when carbon prices exceed 50–100 €/t CO_2.

Credit author statement

M.E. Diego: Conceptualization, Methodology, Investigation, Formal analysis, Writing - original draft, Writing -review & editing. J.C. Abanades: Conceptualization, Methodology, Investigation, Project administration

Declaration of competing interest

The authors declare that they have no known competing financial interests or personal relationships that could have appeared to influence the work reported in this paper.

Acknowledgements

M.E. Diego acknowledges the award of a "Juan de la Cierva-Incorporación" contract from the Spanish MICINN.

Appendix

The design of the novel back-up chemical looping reactor of Tables 1 and 2 basically involves decisions on the total oxygen carrier mass stored in the reactor (depending on the expected maximum power output, the time of the power discharge and material properties such as maximum level of conversion, oxygen carrying capacity, etc.), gas conduct dimensions and wall characteristics to ensure sufficient fluxes of oxygen towards the solids and quality heat transfer from the wall to the air, reactor length and cross sections to accommodate the space occupied by the empty gas conducts and their metallic walls, as well as the packed bed of solids. The overall mass and energy balances in the reactor to align these decisions require a quantitative description of the O_2 diffusion flows through orifices in perforated walls, which ultimately determines the thermal power generated per gas conduct and unit length. These relationships have been recently published elsewhere [18] for a particular application of the reactor in chemical looping combustion systems and therefore, they are only briefly explained here.

First, considering the notation and O_2 transport mechanism depicted in Fig. 2, it is assumed that the kinetics of the oxidation reaction when O_2 reaches the vicinity of the oxydising particles is much faster than the diffusion of O_2 towards the particles, as this is deliberately hindered due to the presence of the perforated wall. We ignore for simplicity the additional diffusion resistance that may appear as the oxidation front departs perpendicularly from the gas conduct wall as the discharge stage progresses (see Ref. [18] for a case including such possibility). Therefore, all reduced particles in the bed of solids particles are assumed to act as an O_2 sink and the concentration of O_2 at the vicinity of the solids is taken to be zero. In these conditions, the O_2 diffusion flow towards the reacting solids and therefore, the overall oxidation reaction, is only limited by the restrictions imposed by the perforated wall. Fick's law governs the O_2 flow through the orifices in the wall at any length z in the reactor and any given time:

$$N_{O_2,z} = \frac{D_{O_2,z}\, A_w \in_w C_{O_2,z}}{l_0} \tag{A.1}$$

where $N_{O2,z}$ is the local molar flow of O_2 that diffuses through the orifices, $D_{O2,z}$ is the local O_2 diffusivity, A_w is the total wall area, ε_w is the fraction of orifices per wall area (assumed to be equal along the reactor), l_0 is the length of the orifices (wall thickness) and $C_{O2,z}$ is the local O_2 concentration in the gas conduct (see Fig. 2).

Gas and wall temperatures can be calculated along the reactor by means of an energy balance applied to an adiabatic differential volume. Absence of radial temperature profiles is assumed in both the solids and the perforated wall, due to the expected low thickness of the solids bed in between the gas conducts and the high conductivity of the perforated wall. Therefore, the heat released at particle level during the oxidation is transferred through the bed of solids and the wall to heat up the gas:

$$N_{O_2,z}\Delta H_{ox,O2} = h_{w,z}A_w(1-\in_w)\left(T_{w,z}-T_{gas,z}\right) = \int m_{gas,z}c_{P\ gas,z}dT_{gas} \tag{A.2}$$

where $\Delta H_{ox,O2}$ is the oxidation enthalpy per mol of O_2, $T_{w,z}$ and $T_{gas,z}$ are the local wall and gas temperatures, $m_{gas,z}$ is the local mass flow of gas and $c_{Pgas,z}$ is the heat capacity of the gas at a reactor length z. The local heat transfer coefficient of the wall, $h_{w,z}$, can be calculated based on the Nusselt

number, using the diameter of the gas conduct, D_c, and the conductivity of the gas, k:

$$h_{w,z} = \frac{Nu_z\ k}{D_c} \tag{A.3}$$

Finally, the pressure drop of the gas in the gas conducts across the reactor can be calculated on the basis of the fanning factor, which can be obtained as a function of the Reynolds number by means of the following expression [31]:

$$f_{F,z} = \frac{0.04}{Re_z^{0.16}} \tag{A.4}$$

References

[1] IPCC. Global warming of 1.5°C. Summary for policymakers. 2018. p. 32.
[2] IRENA. Innovation landscape for a renewable-powered future: solutions to integrate variable renewables. 2019. p. 164.
[3] IEA. World. Energy outlook. 2018. p. 643.
[4] Power IRENA. System flexibility for the energy transition. Part 1: overview for policy makers. 2018. p. 48.
[5] Davis SJ, Lewis NS, Shaner M, Aggarwal S, Arent D, Azevedo IL, et al. Net-zero emissions energy systems. Science 2018;360:1–9.
[6] Gallo AB, Simões-Moreira JR, Costa HKM, Santos MM, Moutinho dos Santos E. Energy storage in the energy transition context: a technology review. Renew Sustain Energy Rev 2016;65:800–22.
[7] California Energy Commission. Thermal efficiency of natural gas-fired generation in California: 2016 update. 2017. p. 40.
[8] US Energy Information Administration. Natural gas-fired combustion turbines are generally used to meet peak electricity load. https://www.eia.gov/todayinenergy/detail.php?id=13191. [Accessed March 2020].
[9] Criado YA, Arias B, Abanades JC. Calcium looping CO_2 capture system for back-up power plants. Energy Environ Sci 2017;10:1994–2004.
[10] Dunn B, Kamath H, Tarascon J-M. Electrical energy storage for the grid: a battery of choices. Science 2011;334:928–35.
[11] SAPEA, Science Advice for Policy by European Academies. Novel carbon capture and utilisation technologies: research and climate aspects. SAPEA Evidence Review Report No 2018;2:95.
[12] IEA. The future of hydrogen. 2019. p. 203.
[13] Andersson J, Grönkvist S. Large-scale storage of hydrogen. Int J Hydrogen Energy 2019;44:11901–19.
[14] Witkowski A, Rusin A, Majkut M, Stolecka K. Comprehensive analysis of hydrogen compression and pipeline transportation from thermodynamics and safety aspects. Energy 2017;141:2508–18.
[15] Hepburn C, Adlen E, Beddington J, Carter EA, Fuss S, Mac Dowell N, et al. The technological and economic prospects for CO_2 utilization and removal. Nature 2019;575:87–97.
[16] Abanades JC, Rubin ES, Mazzotti M, Herzog HJ. On the climate change mitigation potential of CO_2 conversion to fuels. Energy Environ Sci 2017;10:2491–9.
[17] Fuss S, Canadell JG, Peters GP, Tavoni M, Andrew RM, Ciais P, et al. Betting on negative emissions. Nat Clim Change 2014;4:850–3.
[18] Abanades JC, Diego ME, Fernández JR. A novel air reactor concept for chemical looping combustion systems operated at high temperature. Chem Eng J 2020;390:124507.
[19] Noorman S, van Sint Annaland M, Kuipers. Packed bed reactor technology for chemical-looping combustion. Ind Eng Chem Res 2007;46:4212–20.
[20] Noorman S, Gallucci F, van Sint Annaland M, Kuipers HJAM. Experimental investigation of a CuO/Al_2O_3 oxygen carrier for chemical-looping combustion. Ind Eng Chem Res 2010;49:9720–8.
[21] Noorman S, Gallucci F, van Sint Annaland M, Kuipers JAM. A theoretical investigation of CLC in packed beds. Part 2: reactor model. Chem Eng J 2011;167:369–76.
[22] Spallina V, Gallucci F, Romano MC, Chiesa P, Lozza G, van Sint Annaland M. Investigation of heat management for CLC of syngas in packed bed reactors. Chem Eng J 2013;225:174–91.
[23] Spallina V, Chiesa P, Martelli E, Gallucci F, Romano MC, Lozza G, et al. Reactor design and operation strategies for a large-scale packed-bed CLC power plant with coal syngas. Int J Greenh Gas Con 2015;36:34–50.
[24] Fernández JR, Abanades JC. Conceptual design of a Ni-based chemical looping combustion process using fixed-beds. Appl Energy 2014;135:309–19.
[25] Fernández JR, Alarcón JM. Chemical looping combustion process in fixed-bed reactors using ilmenite as oxygen carrier: conceptual design and operation strategy. Chem Eng J 2015;264:797–806.
[26] Gonzalez-Salazar MA, Kirsten T, Prchlik L. Review of the operational flexibility and emissions of gas- and coal-fired power plants in a future with growing renewables. Renew Sustain Energy Rev 2018;82:1497–513.
[27] Siemens. Industrial Gas Turbines. https://new.siemens.com/global/en/products/energy/power-generation/gas-turbines.html. [Accessed March 2020].
[28] Swedish Gas Technology Centre. Basic data on biogas. 2012.
[29] Scarlat N, Dallemand J-F, Fahl F. Biogas: developments and perspectives in europe. Renew Energy 2018;129:457–72.
[30] Jerndal E, Mattisson T, Lyngfelt T. Thermal analysis of chemical-looping combustion. Chem Eng Res Des 2006;84(A9):795–806.
[31] Perry RB, Green DW. Perry's chemical engineers. 1999. Handbook.
[32] Guandalini G, Romano MC, Ho M, Wiley D, Rubin ES, Abanades JC. A sequential approach for the economic evaluation of new CO_2 capture technologies for power plants. Int J Greenh Gas Con 2019;84:219–31.
[33] Mancuso L, Cloete S, Chiesa P, Amini S. Economic assessment of packed bed chemical looping combustion and suitable benchmarks. Int J Greenh Gas Con 2017;64:223–33.
[34] Riva L, Martínez I, Martini M, Gallucci F, van Sint Annaland M, Romano MC. Techno-economic analysis of the Ca-Cu process integrated in hydrogen plants with CO_2 capture. Int J Hydrogen Energy 2018;43:15720–38.
[35] DOE/NETL. Current and future technologies for natural gas combined cycle (NGCC) power plants. 2013. p. 235.
[36] DOE. Cost and performance baseline for fossil energy plants, vol. 1. Bituminous Coal and Natural Gas to Electricity; 2019. p. 577.
[37] IRENA. Biogas for road vehicles: technology brief. 2017. p. 60.